

Determination of the fermion pair size in a resonantly interacting superfluid

Christian H. Schunck, Yong-il Shin, André Schirotzek, and Wolfgang Ketterle

Department of Physics, MIT-Harvard Center for Ultracold Atoms, and Research Laboratory of Electronics, MIT, Cambridge, MA 02139

(Dated: February 4, 2008)

Fermionic superfluidity requires the formation of pairs. The actual size of these fermion pairs varies by orders of magnitude from the femtometer scale in neutron stars and nuclei to the micrometer range in conventional superconductors. Many properties of the superfluid depend on the pair size relative to the interparticle spacing. This is expressed in BCS-BEC crossover theories [1, 2, 3], describing the crossover from a Bardeen-Cooper-Schrieffer (BCS) type superfluid of loosely bound and large Cooper pairs to Bose-Einstein condensation (BEC) of tightly bound molecules. Such a crossover superfluid has been realized in ultracold atomic gases where high temperature superfluidity has been observed [4, 5]. The microscopic properties of the fermion pairs can be probed with radio-frequency (rf) spectroscopy. Previous work [6, 7, 8] was difficult to interpret due to strong and not well understood final state interactions. Here we realize a new superfluid spin mixture where such interactions have negligible influence and present fermion-pair dissociation spectra that reveal the underlying pairing correlations. This allows us to determine the spectroscopic pair size in the resonantly interacting gas to be $2.6(2)/k_F$ (k_F is the Fermi wave number). The fermions pairs are therefore smaller than the interparticle spacing and the smallest pairs observed in fermionic superfluids. This finding highlights the importance of small fermion pairs for superfluidity at high critical temperatures [9]. We have also identified transitions from fermion pairs into bound molecular states and into many-body bound states in the case of strong final state interactions.

The properties of pairs are revealed in a dissociation spectrum, where pair dissociation is monitored as a function of the applied energy E . The spectrum has a sharp onset at the pair's binding energy E_b , where the fragments have zero kinetic energy, and then spreads out to higher energy. Since a rf photon has negligible momentum, the allowed momenta for the fragments reflect the Fourier transform $\Phi(k)$ of the pair wavefunction $\phi(r)$, which has a width on the order of $1/\xi$ where ξ is the pair size. Thus the pair size can be estimated from the spectral line width E_w as $\xi^2 \sim \hbar^2/mE_w$ (m is the mass of the particles and \hbar is Planck's constant h divided by 2π).

The conceptually simplest pairs in the BCS-BEC crossover are the weakly bound molecules in the BEC limit, which are described by a spatial wavefunction $\phi_m(r) \propto e^{-r/b}/r$ with a binding energy $E_b = \hbar^2/mb^2$. When the molecules are dissociated into non-interacting free particles, the spectral response is $I_m \propto \sqrt{E - E_b}/E^2$, showing a highly asymmetric line shape with a steep rise at the molecular binding energy E_b and a long "tail" to higher energies (Fig. 1a) [5, 10].

This general behavior of the dissociation spectrum holds also in the BCS limit where pairing is a many-body effect [5, 11]. The rf dissociation process discussed below, in the limit of negligible final state interactions, can be considered as breaking a Cooper pair into one quasiparticle and one free particle. The rf spectrum in the BCS limit has an onset at $\Delta^2/2E_F$ and the same dependence of $E^{-3/2}$ at high energy as in the BEC limit (Fig. 1b; here E_F is the Fermi energy and Δ is the gap) [12]. Since the rf excitation takes place throughout the whole Fermi sea it is most natural to interpret the BCS state as $N/2$ pairs

with condensation energy $\Delta^2/2E_F$ where N is the total number of fermions [5].

A spectroscopic pair size can be defined both from the onset and the width of the rf spectrum as $\xi_{th}^2 = \hbar^2/2mE_{th}$ and $\xi_w^2 = \gamma \times \hbar^2/2mE_w$. Here E_{th} is the onset/threshold energy, E_w is the full width at half maximum, and $\gamma = 1.89$ is a numerical constant chosen for convenience (see caption of Fig. 1). The pair sizes ξ_{th} and ξ_w which can be directly obtained from the rf spectrum capture the evolution of the pair size from the BCS limit to the BEC limit (see Fig. 1c).

Since the rf spectra show a similar behavior in both limiting cases of the BEC-BCS crossover, one would expect comparable spectra within the crossover regime. Surprisingly, the rf spectra obtained in previous rf experiments did not fit into this picture: the lineshape did not show any pronounced asymmetry and the linewidth was narrow [6, 7, 8] (see also Fig. 7). These experiments could therefore not be simply interpreted in terms of pairing energy and pair size. We will show that this is caused by strong final state interactions and transitions to bound states.

In the previous and our new experiments, the fermion pairs consist of two atoms in different hyperfine states $|a\rangle$ and $|b\rangle$. The rf transfers atoms in state $|b\rangle$ to an initially unoccupied third state $|c\rangle$. In addition to "pair dissociation", also referred to as a "bound-free" transition and characterized by the asymmetric lineshape discussed above, rf spectroscopy can induce a second kind of transition to another bound state, i.e. the transfer of a pair (a,b) to a pair (a,c) (also referred to as a "bound-bound" transition). The latter spectra have a narrow and symmetric lineshape.

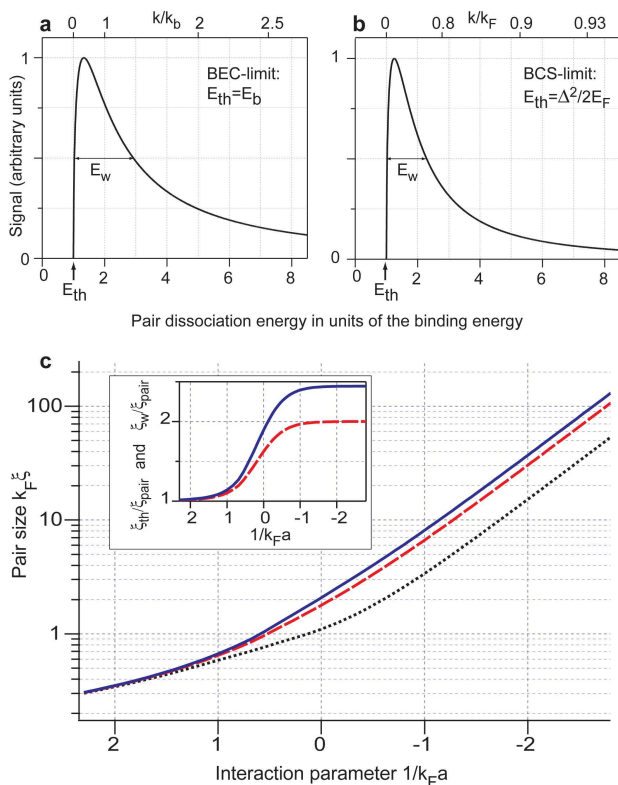


FIG. 1: Line shape of the pair dissociation spectrum in the BEC (a) and BCS limit (b) and the evolution of the fermion pair size in the BEC-BCS crossover [5, 11, 20]. (a) and (b): Simulated rf dissociation spectra in the BEC and BCS limits. The momentum k of the free particles after dissociation is indicated in the top axes, where $\hbar^2 k_b^2/m = E_b$. Apart from an offset, the spectra in the BEC and BCS limits show almost indistinguishable lineshapes. The molecular dissociation lineshape I_m with an additional offset parameter can therefore serve as a generic, model independent fit function for pair dissociation spectra (see Methods and Fig. 6). (c) The fermion pair sizes ξ_w (solid blue) and ξ_{th} (dashed red) are displayed as a function of the interaction parameter $1/k_F a$ (a is the s -wave scattering length). Also shown is the two-particle correlation length ξ_{pair} (dotted black) given by $\xi_{pair} = \sqrt{\langle \phi | r^2 | \phi \rangle / \langle \phi | \phi \rangle}$, where $\phi(r) = \langle \psi | \Psi_\alpha^\dagger(r) \Psi_\beta^\dagger(0) | \psi \rangle$. Here ψ is the generalized BCS wavefunction and α and β refer to the two components [2]. In the BEC limit, the value for the molecular size is $\xi_m = b/\sqrt{2} = \xi_{pair}$. We chose $\gamma = 1.89$ in the definition of ξ_w , so that $\xi_m = \xi_{th} = \xi_w$. In the BCS limit, $\xi_{pair} = \pi/(2\sqrt{2})\xi_c$ where $\xi_c = \hbar^2 k_F / (\pi m \Delta)$ is the Pippard coherence length and we have $\xi_{th} = 2\xi_{pair}$, $\xi_w = 2.44\xi_{pair}$. The inset shows the ratios ξ_w/ξ_{pair} (solid blue) and ξ_{th}/ξ_{pair} (dashed red). Although ξ_{pair} changes by orders of magnitude, ξ_{th} and ξ_w show the same behavior as ξ_{pair} deviating from each other by not more than 22%. This illustrates that the pair size can be reliably determined from the rf dissociation spectrum throughout the whole BEC-BCS crossover.

Final state effects arise when the dissociated atom in state $|c\rangle$ interacts with atoms in state $|a\rangle$. The interaction strength is measured by the dimensionless parameter $k_F a$. Here a is the s -wave scattering length and we use a_i (a_f) for the initial (a,b) (final (a,c)) interactions. As discussed in detail below, final state interactions severely affect the rf dissociation spectra when $|k_F a_f| > 1$ [13, 14, 15]. To overcome this problem, one has to change the interactions in the final state without changing those in the initial one. Our solution is the realization of a new high temperature superfluid in ${}^6\text{Li}$ using a different combination of hyperfine states for which rf excitation with reduced final state interactions is possible (see Methods). As a result, we were able to resolve the bound-bound and bound-free contributions to the rf spectrum, and to determine the size of fermion pairs from the asymmetric fermion pair dissociation spectra.

We have taken advantage of the fact that any two state mixture (1,2), (1,3), and (2,3) of the three lowest hyperfine states of ${}^6\text{Li}$ (labeled in the order of increasing hyperfine energy as $|1\rangle$, $|2\rangle$ and $|3\rangle$) exhibits a broad Feshbach resonance [16, 17]. So far, all experiments with strongly interacting fermions in ${}^6\text{Li}$ have been carried out in the vicinity of the (1,2) Feshbach resonance located at about $B_{12} \sim 834$ G. Surprisingly, inelastic collisions including allowed dipolar relaxation are not enhanced by the (1,3) and (2,3) Feshbach resonances. We observe that at both the (1,3) and (2,3) Feshbach resonances superfluids can be created as well (see Methods). This doubles the number of high temperature superfluids available for experimental studies.

The newly created (1,3) superfluid is the best choice for rf spectroscopy experiments since the final state scattering length a_f at the (1,3) resonance position $B_{13} \sim 691$ G is small and positive ($0 < k_F a_f < 1$ for typical values of k_F). Therefore the accessible final states are either a molecule of a well defined binding energy or two free, only weakly interacting atoms. The actual final state interactions depend on whether one drives the rf transitions from $|1\rangle$ to $|2\rangle$ or from $|3\rangle$ to $|2\rangle$ allowing the comparison between spectra taken from the same sample but with different a_f (see Methods and Supplementary Information). After preparing the (1,3) superfluid a rf pulse resonant with the $|3\rangle$ to $|2\rangle$ transition is applied. Then either the losses in state $|3\rangle$ or the atoms transferred to state $|2\rangle$ are monitored (see Methods). All spectra are plotted versus frequency or energy relative to the atomic resonance, i.e. relative to the energy E_0 required to transfer an atom from $|3\rangle$ to $|2\rangle$ in the *absence* of atoms in state $|1\rangle$.

The main result of this paper are the spectra observed in the (1,3) BEC-BCS crossover between 670 and 710 G (Fig. 2). The spectra have the asymmetric lineshape characteristic for pair dissociation and are indeed well fit by a generic pair dissociation lineshape convolved with the lineshape of the square excitation pulse (see Fig. 1

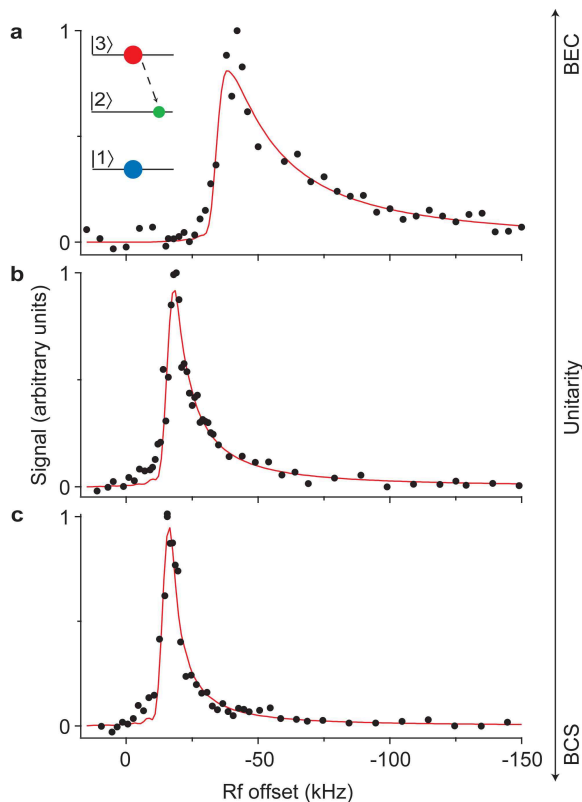


FIG. 2: Rf dissociation spectra in the BEC-BCS crossover. Below, at, and above resonance, the spectrum shows the typical asymmetric lineshape of a pair dissociation spectrum. The signal is proportional to the three dimensional local response at the center of the cloud (see Methods). Since state $|3\rangle$ has a higher energy than state $|2\rangle$ (see the schematic inset in (a)), the dissociation energy is always less than the transition frequency for the atomic resonance E_0/h and therefore the dissociation spectra appear at negative energies compared to E_0 . The inverted frequency axis ensures that the dissociation spectrum is always on the right (or “positive”) side of the origin. The magnetic field (in G), the local Fermi energy ϵ_F (in kHz), the temperature T in units of the Fermi temperature T/T_F and the interaction strength $1/k_F a_i$ are (a), 670, $h \times 24$, ≈ 0.2 , 0.4; (b), 691, $h \times 21$, 0.1, ~ 0 ; (c), 710, $h \times 20$, 0.1, -0.3.

and Methods). If the frequency axis is scaled by E_w and the spectra are shifted to show the same onset all three spectra overlap as shown in Fig. 3a. At the level of our experimental resolution the dissociation lineshape is therefore not sensitive to a change in interactions. As illustrated in Fig. 1, the pair size can in principle be obtained from both E_{th} and E_w . However, since the whole spectrum may be subject to shifts from Hartree terms [16, 18], we focus in the following only on the width of the spectrum.

At unitarity we determine the full width at half maximum to be $E_w = 0.28(5)\epsilon_F$ corresponding to a spectroscopic pair size of $\xi_w = 2.6(2)/k_F$ (here ϵ_F is the local Fermi energy and $k_F = \sqrt{2m\epsilon_F}/\hbar$; the quoted errors are purely statistical). The pairs are therefore smaller than the interparticle spacing l given by $l = n^{1/3} = (3\pi^2)^{1/3}/k_F \sim 3.1/k_F$ (where n the total density) and in units of $1/k_F$ the smallest reported so far for fermionic superfluids. In high-temperature superconductors the reported values for ξ at optimal doping are in the range of

5 to $10/k_F$ [9].

In the simple BEC-BCS crossover model the ratio ξ_{pair}/ξ_w varies from 1 to $1/2.4$. The fact that ξ_w is smaller than l suggests the use of the molecular ratio, i.e. $\xi \equiv \xi_{pair} = \xi_w = 2.6/k_F$. Before we compare with theoretical predictions we note that various definitions of the pair size differ by factors on the order of unity [19]. With this in mind, we find that our observed ξ is larger than a predicted pair size of about $1/k_F$ based on a functional integral formulation of the BEC-BCS crossover [20]. Small fermion pair sizes have been explicitly linked to high critical temperatures via the relation $T_c/T_F \approx 0.4/(k_F \xi_{pair})$ which applies for weak coupling [9]. Inserting the observed ξ this relation yields an estimate of $T_c/T_F \approx 0.15$ which is in the range of the predicted values between 0.15 to 0.23 (here T_F is the local Fermi temperature) [21]. If we use the asymptotic BCS relation $\Delta = \frac{\hbar^2 k_F}{\pi m} \frac{1}{\xi_c} = \frac{1}{\sqrt{2}} \frac{1}{k_F \xi_{pair}} \epsilon_F$, valid at weak coupling, and our observed ξ at unitarity we find $\Delta \approx 0.3\epsilon_F$ smaller than the value of $0.5\epsilon_F$ predicted by Monte Carlo

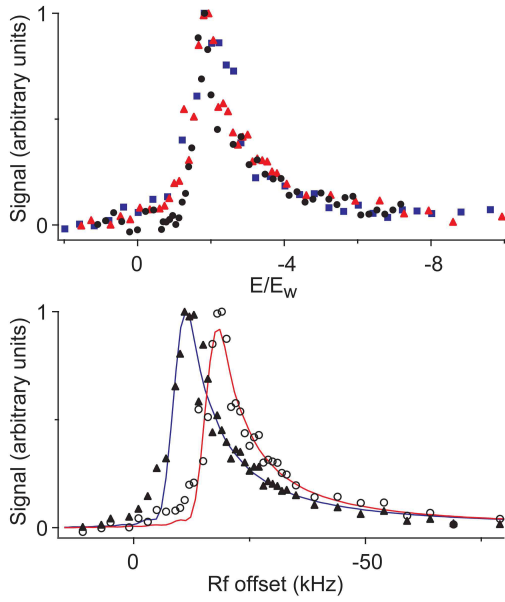


FIG. 3: Comparison of lineshapes and density effects. (a) Same spectra as in Fig. 2 but with the frequency axis scaled by E_w and shifted so that the spectral onsets overlap with the BEC side spectrum: BEC side (black circles), resonance (red triangles), and BCS side (blue squares). (b) Density effects at unitarity for the (1,3) mixture at 691 G. The figure shows the tomographically reconstructed spectral response in the center (open circles, same spectrum as in Fig. 2b) as well as the lower density wings (filled triangles) of the cloud. In this regime the cloud might have turned normal.

simulations [22].

The strong narrowing of the spectral line in Fig. 2 (a) to (c) demonstrates that the fermion pair size increases from strong to weak coupling. The decreasing width corresponds to a more than twofold increase of the spectroscopic pair size from $\xi_w = 1.4(1)/k_F$ at 670 G to $\xi_w = 3.6(3)/k_F$ at 710 G. A change of the absolute pair size with density at unitarity can in principle be observed by comparing the spectral width in the center and the outer region of the cloud. As the density decreases, the spectral onset also becomes increasingly softer and the asymmetry of the pair dissociation peak less pronounced, possibly due to atomic diffusion during the excitation pulse. This prevents a reliable determination of the pair size in the spatial wings where the density is changing rapidly.

We now consider the effect of final state interactions in more detail. First we would like to point out that the increase in a_f by about a factor of two from 670 G to 710 G has not affected the lineshape of the spectra in Fig. 3a within the experimental resolution. This suggests that final state effects are small for these spectra. Additional information is obtained from the previously introduced bound-bound (BB) transitions which are outside

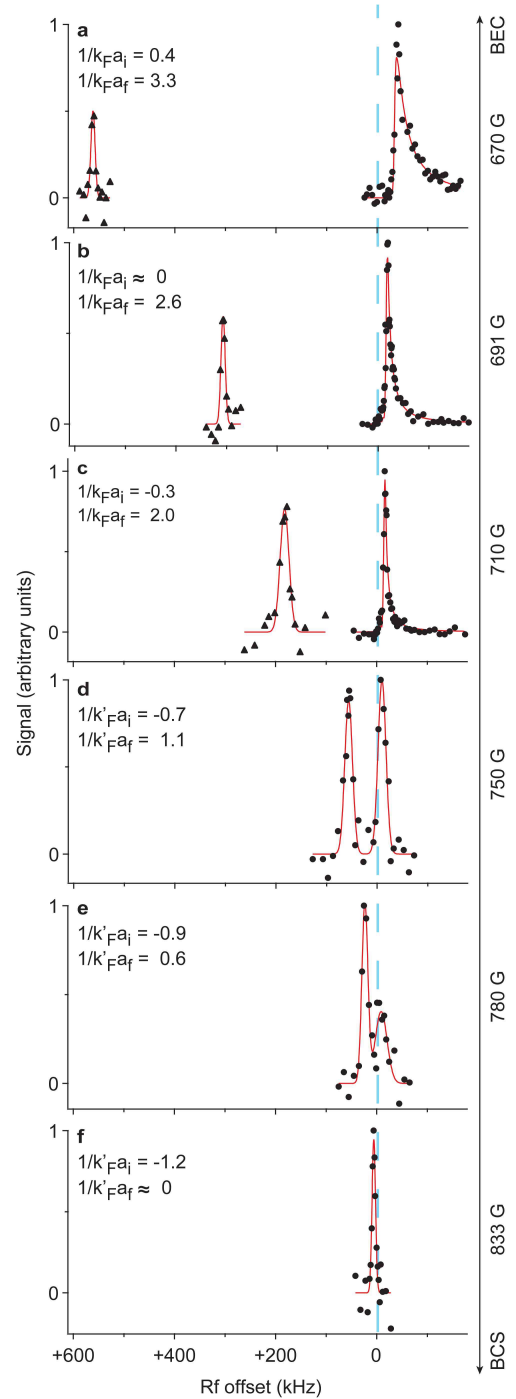


FIG. 4: Effect of final state interactions on rf spectroscopy: bound-bound (BB) and bound-free (BF) spectra in the BEC-BCS crossover of the (1,3) mixture (only the BF spectra in (a-c) were tomographically reconstructed). While the initial (1,3) state is strongly interacting at all fields the final state interactions change from weak (a-c) to strong (d-f). See ref. [17] for a plot of the Feshbach resonances. At the higher magnetic fields for $1/k_F a_i \approx -1$ the initial state may have turned normal. (a-c), Same BF spectra and parameters as in Fig. 2. The relative weight of the BB and BF peaks could not be determined experimentally (see Methods). (d), 750 G, $E_F = h \times 22$ kHz, $T/T_F = 0.09$; (e), 780 G, $E_F = h \times 23$ kHz, $T/T_F = 0.09$; (f), 833 G, $E_F = h \times 20$ kHz, $T/T_F = 0.06$.

the range plotted in Fig. 2. On the BEC side of the resonance the (1,3) molecule can be transferred also to a more deeply bound (1,2) molecule (see Fig. 4a). The BB peak is still present at unitarity and also on the BCS side at 710 G (Fig. 4b and c) and results from the transition of a many-body bound fermion pair to a (1,2) molecule. The strong overlap of the pair wavefunction and the molecule in the final state is another indication for the “molecular” character of the fermions pairs in the strongly interacting regime.

The spectra start to change significantly at higher fields. As the magnetic field is increased the (1,3) mixture remains in the unitarity limited regime with the interaction strength approaching $1/|k_F a_i| \approx 1$ at $B_{12} = 833$ G. The final state interactions, however, change from weak to strong causing the pair dissociation peak to decrease in weight and the BB peak to become dominant (Fig. 4d-f). This single peak apparently corresponds to a BB transition from many-body bound (1,3) pairs to a highly correlated final state of an atom in state $|2\rangle$ interacting with the paired atoms in state $|1\rangle$.

A narrow BB peak is predicted both in the molecular (two-body) and many-body case, when initial and final state interactions are identical or similar. The spectra in Fig. 4 show that BB transitions dominate when $|1/(k_F a_i) - 1/(k_F a_f)| \leq 1.5$. In our opinion a recent theoretical treatment [23] agrees qualitatively with these results but underestimates the region where BB transitions are dominant by about a factor of two. Our observations allow a reinterpretation of the rf spectra obtained from the (1,2) superfluid with resonant interactions [6, 7, 8] (see the Supplementary Information for an extended discussion). The spectra have been taken in a regime where $|1/(k_F a_i) - 1/(k_F a_f)| \leq 1$ where strong BB transitions are expected. Together with the very narrow and symmetric lineshape (see Fig. 7), this suggests that the (1,2) to (1,3) rf spectra at 833 G are dominated by such BB transitions and cannot be simply interpreted in terms of a pair dissociation process and a pairing gap [6, 7, 8, 24, 25, 26].

In conclusion we have determined the pair size of resonantly interacting fermions using new superfluid spin mixtures in ${}^6\text{Li}$. The (1,3) mixture is ideally suited for rf spectroscopy since final state interactions do not significantly affect the spectra. Our measurements are the first to clearly reveal the microscopic structure of the fermion pairs in the strongly interacting regime. The small fermion pair size and high critical temperatures observed in our system show a relation similar to the one suggested by the Uemura plot for a wide class of fermionic superfluids [9]. Our results also explain why the rapid ramp method used to observe fermion pair condensation in the crossover has been successful [27, 28]. The small pair size facilitated the efficient transfer of the many-body bound fermion pairs into more strongly bound molecules while preserving the momentum distri-

bution of the pairs.

This work opens ample opportunities for future research. The microscopic structure of the pairs can now be studied both in the superfluid and normal phase as a function of interaction strength, temperature and spin imbalance between the two components [7]. Increased spectral resolution may reveal interesting deviations of the spectral shape from the generic lineshape discussed here. Furthermore, the predicted universality of a resonantly interacting Fermi mixture can now be tested in ${}^6\text{Li}$ for three different systems. The lifetimes of all three two-state combinations of the three lowest hyperfine states in ${}^6\text{Li}$ are on the order of 10 s in the strongly interacting regime. The three-body decay rates, however, decrease by more than an order of magnitude between 690 and 830 G for a ternary mixture, which may reflect interesting three-body physics. The lifetime of 30 ms at 691 G might be sufficient for studies involving all three hyperfine states [29] with the potential for experiments on pairing competition in multi-component Fermi gases and spinor Fermi superfluids.

We thank M. Zwierlein, W. Zwerger, E. Mueller and S. Basu for stimulating discussions and A. Keshet for the experiment control software. This work was supported by the NSF and ONR, through a MURI program, and under ARO Award W911NF-07-1-0493 with funds from the DARPA OLE program.

Methods Summary

Creation of the (1,3) superfluid. As described previously [5] a spin polarized sample of ultracold ${}^6\text{Li}$ in state $|1\rangle$ is obtained in an optical dipole trap after sympathetic cooling with ${}^{23}\text{Na}$ in a magnetic trap. The equal (1,3) mixture is prepared at 568 G, close to the zero crossing of a_{13} . Here a non-adiabatic Landau-Zener rf sweep, creating an equal (1,2) mixture, is followed by an adiabatic Landau-Zener sweep that transfers the atoms in state $|2\rangle$ to state $|3\rangle$. To induce strong interactions the magnetic field is adjusted in 100 ms to 730 G and then ramped to values between 660 and 833 G. After evaporative cooling in the optical trap, superfluidity is indirectly established via the observation of fermion pair condensates [27, 28]. Under comparable conditions quantized vortex lattices, a direct proof for superfluidity, have been observed in the rotating (1,2) mixture of ${}^6\text{Li}$ [4]. $E_F = \hbar(\nu_r^2 \nu_{ax})^{1/3} (3N)^{1/3}$ with radial (axial) trapping frequencies $\nu_r = 140$ ($\nu_{ax} = 22$) Hz and $k'_F = \sqrt{2mE_F}/\hbar$. The temperature was determined from the shape of the expanded cloud.

Recording the (1,3) rf spectra. The rf dissociation spectra at 670, 691 and 710 G spectra have been obtained by applying a 200 μs long rf pulse to the (1,3) mixture monitoring the atoms transferred into state $|2\rangle$. Three-dimensional image reconstruction via the inverse Abel transformation was used to obtain local rf dissociation

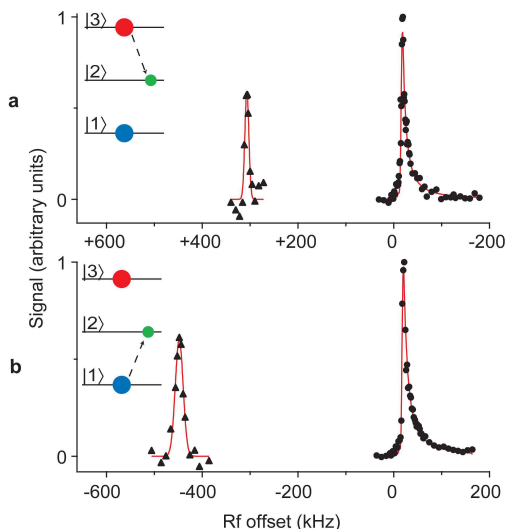


FIG. 5: Rf spectra at unitarity for the (1,3) mixture at 691 G. For all spectra the number of atoms transferred to state $|2\rangle$ has been recorded. In the (1,3) mixture rf transitions to the final state $|2\rangle$ are possible from both states $|1\rangle$ and $|3\rangle$. The final states can therefore be either bound (2,3) or (1,2) molecules respectively or a dissociated free atom in state $|2\rangle$. Note that the bound-free (BF) spectra are very similar for both $|3\rangle$ to $|2\rangle$ (a) and $|1\rangle$ to $|2\rangle$ (b) transitions. The bound-bound (BB) spectra, however, show different shifts indicating that the final (2,3) molecule is more strongly bound than the (1,2) molecule. This is a consequence of the smaller width of the (2,3) Feshbach resonance at 811 G [17] compared to the width of the (1,2) resonance at 834 G. (a) $|3\rangle$ to $|2\rangle$ transition; $\epsilon_F = 21$ kHz, $T/T_F=0.1$ (b) $|1\rangle$ to $|2\rangle$ transition; $\epsilon_F = 22$ kHz, $T/T_F=0.14$.

spectra [8]. The pulse length was chosen to be shorter than $1/4$ trapping period to minimize atomic diffusion during the excitation pulse. The rf power was adjusted to transfer less than 5% of the total number of atoms. A further reduction of the rf power only affected the signal to noise ratio but not the spectral width. All BB spectra and the spectra at fields at and above 750 G are not spatially resolved and were obtained with about 1 ms long rf pulses.

Full methods

Creation of new superfluid spin mixtures for rf spectroscopy. For the well established (1,2) mixture, only the $|2\rangle$ to $|3\rangle$ transition has been used for rf spectroscopy. The final state s -wave scattering length a_{13} at B_{12} is large and negative leading to strong final state interactions with $1/k_F a_f < -1$ ($a_{13} \approx -3300 a_0$, a_0 the Bohr radius and a_{ij} the magnetic field dependent scattering length between atoms in states $|i\rangle$ and $|j\rangle$). The strength of the final state interactions can in principle be changed in several ways without affecting the initial state. The density could be lowered to reduce the interaction strength in the final state while the initial state

remains resonantly interacting. It is, however, experimentally difficult to decrease the density by a large factor and maintain the same low temperature T/T_F . One might also try to spectroscopically access a different final state. However, in ${}^6\text{Li}$ there are no other allowed magnetic field insensitive transitions. Magnetic field insensitivity is necessary to obtain the required spectral resolution in the kHz regime.

Since other mixtures of hyperfine states in ${}^6\text{Li}$ also exhibit broad Feshbach resonances we attempted to create resonantly interacting superfluids in new combinations of initial hyperfine states: (1,3) and (2,3). The lifetimes of these spin mixtures at resonance exceed 10 s implying inelastic collision rates smaller than $10^{-14} \text{ cm}^{-3} \text{ s}^{-1}$. While for the (2,3) superfluid the final state interactions are also large and negative, the final state scattering lengths at B_{13} are either $a_{23} \approx 1140 a_0$ and $a_{12} \approx 1450 a_0$ (depending on the rf transition employed) and therefore considerably smaller and positive.

Creation of the (2,3) superfluid. To prepare a (2,3) superfluid we follow essentially the same procedure as previously described for the (1,2) mixture [4, 5]. The only difference is that instead of applying a Landau-Zener transfer that creates an equal (1,2) mixture a complete transfer into state $|2\rangle$ is followed by a second sweep creating an equal (2,3) mixture. The final magnetic field at the center of the (2,3) resonance is $B_{23} \approx 811$ G. As in the other spin mixtures we observe fermion pair condensation after evaporation in the optical trap.

Recording the (1,3) spectra: stability of the mixture after the rf pulse Recording the atoms transferred to state $|2\rangle$ is advantageous because there is no background without rf pulse, but it requires that their lifetime with respect to three-body recombination is sufficiently long.

For fields below ~ 710 G, we found that the lifetime of the $|2\rangle$ atoms after the rf pulse was short when they formed a molecule with an $|1\rangle$ atom as the result of a BB transition. Therefore, in some cases, the BB part of the spectra was recorded by observing atom number loss in the initial state. After BF (bound-free) excitation, the lifetime of atoms in state $|2\rangle$ was 30 ms (determined at 691 G) sufficiently long to observe the atoms directly. As a result of the different decay times and recording methods the relative signal strength between the BB and BF parts of the spectrum could not be determined.

At fields above ~ 750 G, we found similar and strong losses after both BF and BB excitations. Therefore all data were taken by monitoring losses in the initial state $|3\rangle$ and the spectra reflect the relative strength between BB and BF transitions.

Fitting the (1,3) spectra The fit to the (1,3) rf dissociation spectra in Figures 2, 3, 4(a-c), 5, and 7 uses a generic, model independent pair dissociation line-shape based on I_m with an additional parameter E_{offset} : $I_{\text{generic}}(E) \propto \sqrt{(E - E_{th}) / (E - E_{\text{offset}})^2}$. We used this

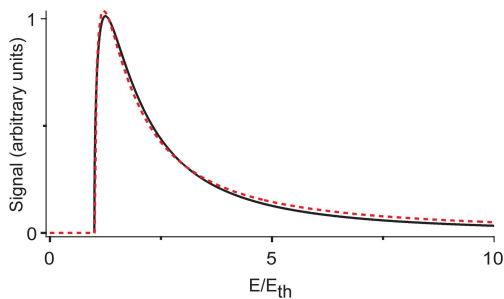


FIG. 6: Generic pair dissociation lineshape. A simulated rf dissociation spectrum in the BCS limit (black solid line) [5] is fit with I_{generic} (red dashed line) which is the molecular lineshape I_m with an additional offset parameter E_{offset} (see Methods).

lineshape convolved with the Fourier transform of the square pulses as a fitting function, and found good agreement with the experimentally obtained spectra shown in Fig. 2. The generic fit function contains no corrections for final state interactions. In the BEC limit (where $E_{\text{offset}} = 0$ and $E_{th} = E_b$) such corrections can be included by a multiplicative factor of $1/(E + \hbar^2/(ma_f^2) - E_{th})$ [30]. When applied to the dissociation spectra in the crossover this correction factor changes the fit only by a negligible amount. All BB and BF spectra in Fig. 4(d-f) have been fit by a Gaussian.

(1,3) mixture: $|3\rangle$ to $|2\rangle$ vs $|1\rangle$ to $|2\rangle$ transition

The (1,3) superfluid gives us the opportunity to record two different (magnetic field insensitive) rf spectra: from state $|3\rangle$ to state $|2\rangle$ (the transition used for all the spectra shown in the paper) and from state $|1\rangle$ to state $|2\rangle$. This allows us to compare rf spectra of the same system but for somewhat different final state interactions. The final state scattering lengths at B_{13} are $a_{23} \approx 1140 a_0$ for the $|1\rangle$ to $|2\rangle$ transition and $a_{12} \approx 1450 a_0$ for the $|3\rangle$ to $|2\rangle$ transition. Figure 5 shows the spectra at 691 G. Note that the fermion pair size obtained from the spectra agrees for both rf transitions within the experimental uncertainty.

Supplementary Information

Final state interactions in the rf spectroscopy experiments with the (1,2) and (1,3) mixtures.

Figure 7 shows the dramatic effect of final state interactions in the (1,2) mixture at unitarity. The narrow and symmetric lineshape observed in the (1,2) to (1,3) rf spectrum suggests that this spectral peak is dominated by a bound-bound (BB) transition from (1,2) pairs to a (1,3) correlated state.

In the molecular case final state interactions can be included in an analytical model [30]. The final states for dissociation are two atoms with momentum $\hbar k$ in an s -wave scattering state with scattering length a_f . For

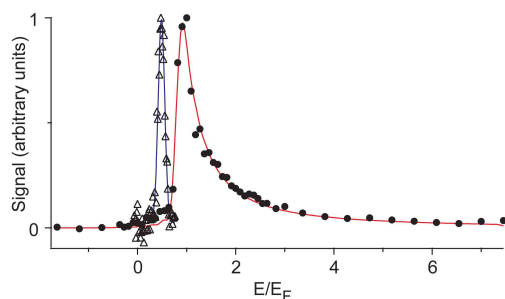


FIG. 7: Comparison of the rf spectra of the (1,2) and (1,3) superfluids at unitarity, showing dramatic final state effects for the (1,2) mixture. Open circles: same rf dissociation data as in Fig. 5b. Solid diamonds: rf spectra at unitarity for the (1,2) mixture at 833 G from ref. [8]. The frequency axis is normalized by the local Fermi energies. In the (1,2) mixture final state effects lead to a strong suppression of the asymmetric “tails” of the rf spectrum and a shift of the peak to lower energies.

a large and positive $a_i \approx b$ and an increasing a_f ($0 < a_f < a_i \approx b$) the dissociation spectrum loses in weight and narrows as $(1 - a_f/a_i)/(1 + k^2 a_f^2)$ until it disappears when a_f/a_i approaches one. At this point the spectrum consists of a delta function for the BB transition between molecular states of equal size.

A very similar behavior of the BB and bound-free (BF) parts of the spectrum is expected for a superfluid with resonant interactions [23]: for $|a_f|, |a_i| \gg 1/k_F$ the spectrum is reduced to a delta function. Here, the initial state is a fermion pair condensate described by the BEC-BCS crossover wavefunction [5, 23]. In contrast to the molecular case, the spectrum of the superfluid at resonance shows a BB peak even for negative values of $1/k_F a_f$, i.e. in a regime where binding is only due to many-body effects [23]. The spectra in Fig. 4 show that BB transitions dominate when $|1/(k_F a_i) - 1/(k_F a_f)| \leq 1.5$ (a region that is about a factor of two larger than obtained in ref. [23]). We also infer from [23] that it is much more difficult to spectrally resolve BB and BF transitions for a system in the unitarity limit if $a_f < 0$. When one approaches resonance for the (1,2) system from the BEC side the BF spectrum narrows and smoothly turns into a BB dominated spectrum.

Compared to the (1,2) superfluid, a_f in the (1,3) system is up to three times smaller and positive. This leads, both in the molecular model (due to the quadratic dependence on $k_F a_f$) and in the resonant case [23], to a dramatic change in the dissociation spectrum towards the limit of negligible final state interactions. Fits to the (1,3) dissociation spectrum both with and without a correction factor for final state effects (see Methods) [30] show negligible differences, indicating the small influence of final state interactions. In fact the (1,3) spectra in Fig. 4(a-c) show the absence of final state effects with-

out any detailed analysis. The splitting between BB and BF parts given by \hbar^2/ma_f^2 is considerably larger than the width of the BF spectrum (which is approximately \hbar^2/mb^2). Therefore the condition $a_f < b$ is fulfilled, implying that final state interactions do not strongly affect the dissociation spectrum.

-
- [1] Eagles, D. M. Possible pairing without superconductivity at low carrier concentrations in bulk and thin-film superconducting semiconductors. *Phys. Rev.* **186**, 456–463 (1969).
- [2] Leggett, A. J. *Modern Trends in the Theory of Condensed Matter*, (eds Pekalski, A. & Przystawa, J.) 13–27 (Proc. XVIth Karpacz Winter School of Theoretical Physics, Springer, Berlin, 1980).
- [3] Nozières, P. & Schmitt-Rink, S. Bose condensation in an attractive fermion gas: from weak to strong coupling superconductivity. *J. of Low Temp. Phys.* **59**, 195–211 (1985).
- [4] Zwierlein, M. W., Abo-Shaeer, J. R., Schirotzek, A., Schunck, C. H. & Ketterle, W. Vortices and superfluidity in a strongly interacting Fermi gas. *Nature* **435**, 1047–1051 (2005).
- [5] Ketterle, W. & Zwierlein, M. W. *Ultracold Fermi Gases*, (eds Inguscio, M., Ketterle, W. & Salomon, C.) 95–287 (Proc. International School of Physics Enrico Fermi, Course CLXIV (IOS Press, Amsterdam, SIF Bologna, 2008).
- [6] Chin, C. *et al.* Observation of the pairing gap in a strongly interacting Fermi gas. *Science* **305**, 1128–1130 (2004).
- [7] Schunck, C. H., Shin, Y., Schirotzek, A., Zwierlein, M. W. & Ketterle, W. Pairing without superfluidity: The ground state of an imbalanced Fermi mixture. *Science* **316**, 867–870 (2007).
- [8] Shin, Y., Schunck, C. H., Schirotzek, A. & Ketterle, W. Tomographic rf spectroscopy of a trapped Fermi gas at unitarity. *Phys. Rev. Lett.* **99**, 090403 (2007).
- [9] Pistolesi, F. & Strinati, G. C. Evolution from BCS superconductivity to Bose condensation: Role of the parameter $k_F\xi$. *Phys. Rev. B* **49**, 6356–6359 (1994).
- [10] Regal, C. A., Ticknor, C., Bohn, J. L. & Jin, D. S. Creation of ultracold molecules from a Fermi gas of atoms. *Nature* **424**, 47–50 (2003).
- [11] Diener, R. B. & Ho, T.-L. The condition for universality at resonance and direct measurement of pair wavefunctions using rf spectroscopy. Preprint, arXiv:cond-mat/0405174v2.
- [12] Yu, Z. & Baym, G. Spin-correlation functions in ultracold paired atomic-fermion systems: Sum rules, self-consistent approximations, and mean fields. *Phys. Rev. A* **73**, 063601 (2006).
- [13] Baym, G., Pethick, C. J., Yu, Z. & Zwierlein, M. W. Coherence and clock shifts in ultracold Fermi gases with resonant interactions. *Phys. Rev. Lett.* **99**, 190407 (2007).
- [14] Punk, M. & Zwerger, W. Theory of rf-spectroscopy of strongly interacting fermions. *Phys. Rev. Lett.* **99**, 170404 (2007).
- [15] Perali, A., Pieri, P. & Strinati, G. C. Competition between final-state and pairing-gap effects in the radio-frequency spectra of ultracold Fermi atoms. *Phys. Rev. Lett.* **100**, 010402 (2008).
- [16] Gupta, S. *et al.* Rf spectroscopy of ultracold fermions. *Science* **300**, 1723–1726 (2003).
- [17] Bartenstein, M. *et al.* Precise determination of ^6Li cold collision parameters by radio-frequency spectroscopy on weakly bound molecules. *Phys. Rev. Lett.* **94**, 103201 (2004).
- [18] Regal, C. A. & Jin, D. S. Measurement of positive and negative scattering lengths in a Fermi gas of atoms. *Phys. Rev. Lett.* **90**, 230404 (2003).
- [19] Ortiz, G. & Dukelsky, J. BCS-to-BEC crossover from the exact BCS solution. *Phys. Rev. A* **72**, 043611 (2005).
- [20] Engelbrecht, J. R., Randeria, M. & Sá de Melo, C. A. R. BCS to Bose crossover: Broken-symmetry state. *Phys. Rev. B* **55**, 15153 – 15156 (1997).
- [21] Burovski, E., Prokof'ev, N., Svistunov, B. & Troyer, M. Critical temperature and thermodynamics of attractive fermions at unitarity. *Phys. Rev. Lett.* **96**, 160402 (2006).
- [22] Carlson, J., Chang, S.-Y., Pandharipande, V. R. & Schmidt, K. E. Superfluid Fermi gases with large scattering length. *Phys. Rev. Lett.* **91**, 050401 (2003).
- [23] Basu, S. & Mueller, E. J. Final-state effects in the radio frequency spectrum of strongly interacting fermions. Preprint, arXiv:0712.1007v2 & private communication.
- [24] Kinnunen, J., Rodríguez, M. & Törmä, P. Pairing gap and in-gap excitations in trapped fermionic superfluids. *Science* **305**, 1131–1133 (2004).
- [25] Ohashi, Y. & Griffin, A. Single-particle excitations in a trapped gas of Fermi atoms in the BCS-BEC crossover region. II. Broad Feshbach resonance. *Phys. Rev. A* **72**, 063606 (2005).
- [26] He, Y., Chen, Q. & Levin, K. Radio-frequency spectroscopy and the pairing gap in trapped Fermi gases. *Phys. Rev. A* **72**, 011602 (2005).
- [27] Regal, C. A., Greiner, M. & Jin, D. S. Observation of resonance condensation of fermionic atom pairs. *Phys. Rev. Lett.* **92**, 040403 (2004).
- [28] Zwierlein, M. W. *et al.* Condensation of pairs of fermionic atoms near a Feshbach resonance. *Phys. Rev. Lett.* **92**, 120403 (2004).
- [29] Honerkamp, C. & Hofstetter, W. Ultracold fermions and the SU(N) Hubbard model. *Phys. Rev. Lett.* **92**, 170403 (2004).
- [30] Chin, C. & Julienne, P. S. Radio-frequency transitions on weakly bound ultracold molecules. *Phys. Rev. A* **71**, 012713 (2005).